

Optical Spectra of Localized Excess Electrons in Alkali Halide Clusters

Gunaretnam Rajagopal, R. N. Barnett, Abraham Nitzan,^(a) and Uzi Landman
School of Physics, Georgia Institute of Technology, Atlanta, Georgia 30332

Eric C. Honea,^(b) Pierre Labastie,^(c) Margie L. Homer, and Robert L. Whetten
Department of Chemistry, University of California at Los Angeles, Los Angeles, California 90024
 (Received 26 February 1990)

Excess electrons attached to small alkali halide clusters give rise to optical-absorption bands whose characteristics are highly specific to the mode of electron localization. Optical spectra measured by cluster beam and resonant two-photon ionization spectroscopy agree well with predictions of coupled classical-quantum simulations, and are interpreted in terms of two localization modes: surface *F*-center and diffuse surface states.

PACS numbers: 71.50.+t, 36.40.+d

Advances in cluster-beam techniques^{1,2} and in theoretical methods^{3,4} have recently yielded substantial new information on the localization modes of excess electrons in molecular clusters,^{3,5} and alkali halide clusters (AHC).^{3,6-9} In the latter case, several modes of localization of electrons attached to clusters consisting of n M^+ alkali-metal ions and m X^- halide ions ($m < n$) have been predicted, depending on the composition of the particular cluster.⁶ Experimental evidence for such

structures has been found.⁸

Specifically, in neutral clusters, M_nX_{n-1} (i.e., $M_n^+X_{n-1}^- \cdot e^-$), which have the requisite number of ions (such as in $\text{Na}_{14}\text{Cl}_{13}$) to form a *filled cubic microlattice* ($2n-1 = j \times k \times l$, with j , k , and l all odd integers denoting the number of ions on the edges of a microcrystalline alkali halide lattice), the excess electron is attached in a *weakly bound surface state* (class I). Other M_nX_{n-1} clusters (where $2n = j \times k \times l$, class II) also form stable

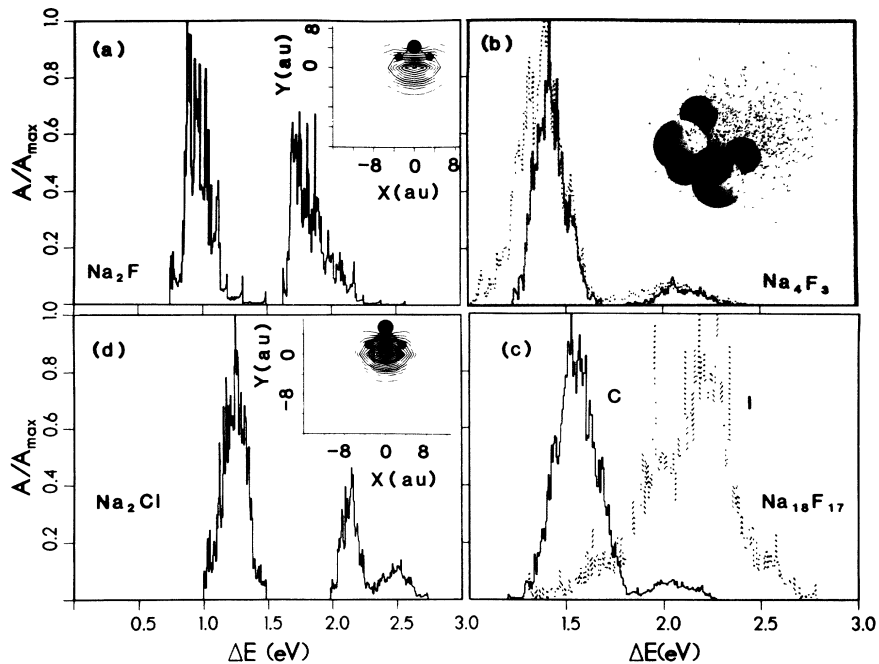


FIG. 1. (a),(b) Calculated spectra for Na_2F (at 100 K) and Na_4F_3 , respectively, using the BH potentials. (b) For Na_4F_3 spectra calculated at 100 K (dashed curve) and 50 K (solid curve) are shown. Insets: (a) Contours of the excess electron density (maximum contour corresponds to $3.089 \times 10^{-3} e/a_0^3$ and the increment between successive contours $\Delta = 2.56 \times 10^{-4}$) in the plane of the Na_2F molecule, and (b) a snapshot of the equilibrium configuration at 100 K of the Na_4F_3 cluster, where the large and small balls correspond to F^- and Na^+ ions, respectively, and the excess electron distribution is represented by the small dots. The geometry of the Na_2F cluster is specified by $d_{\text{Na-F}} = (3.71 \pm 0.11)a_0$, $\theta(\text{Na-F-Na}) = 110.5^\circ \pm 4.0^\circ$, and the distance between the fluorine anion (large filled circle) and the center of the excess electron density $d_{\text{F-e}} = (4.28 \pm 0.15)a_0$. (c) Calculated excess electron spectra for two configurations of the anion vacancy [internal (*I*), dashed curve; corner (*C*), solid curve] of $\text{Na}_{18}\text{F}_{17}$ at 100 K. (d) Calculated spectrum for Na_2Cl at 100 K, using the FT potentials. Inset: Contours of the excess electron density (maximum contour $4.35 \times 10^{-3} e/a_0^3$, $\Delta = 2.724 \times 10^{-4}$). The structural parameters are $d_{\text{NaCl}} = (4.73 \pm 0.09)a_0$, $\theta(\text{Na-Cl-Na}) = 85.7^\circ \pm 2.9^\circ$, and $d_{\text{Cl-e}} = (5.39 \pm 0.08)a_0$.

cuboid structures,^{8,10} with the anion vacancy as a lattice site in which the excess electron localizes (playing the role of the missing X^- ion). This is akin to F -center localization in bulk crystals; thus we call them *surface F -center states*. Clusters which do not have the requisite number of ions to satisfy either of these conditions are noncubic¹⁰ with the electron tending to localize on a particular, weakly bound, M^+ ion (class III).⁶

Optical spectroscopy, in conjunction with theoretical predictions, affords a challenging test of the theoretical models and interaction potentials. This Letter reports on the first extensive, comparative theoretical predictions and experimental observations of spectra of small e -AHC systems ($n < 33$). In particular, calculated spectra for class-II clusters show two strong absorption bands, in the ir and in the red, indicative of a corner site of the electron. For class I only one band is predicted. These predictions are consistent with experimental results, thus providing guidelines for the interpretation of experimental data.

Optical spectra predicted by theoretical simulations are shown for selected clusters in Figs. 1 and 2. The simulation method employs the ground-state dynamics (GSD) version of the time-dependent self-consistent field method.^{11,12} In this method the coupling between the excess electron and the ions is evaluated via the ground-state quantum expectation value of the electron-ion interaction pseudopotential.^{6,13} Throughout the time evo-

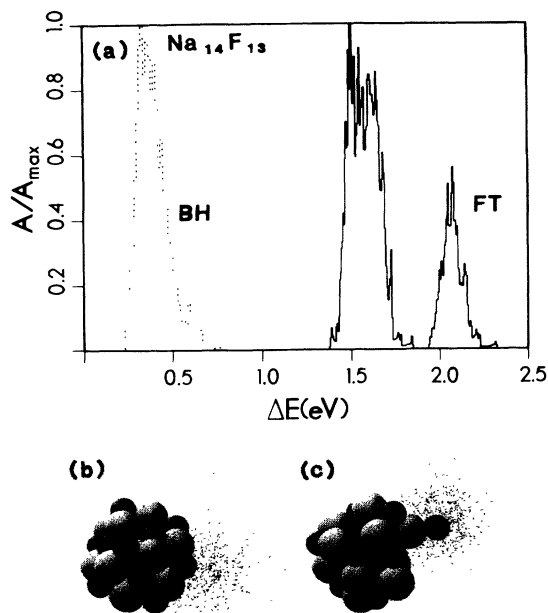


FIG. 2. (a) Calculated spectra for an excess electron surface state in an $\text{Na}_{14}\text{F}_{13}$ cluster at 100 K. Results obtained via the BH and FT potentials are given by dashed and solid curves, respectively. (b),(c) Snapshots of equilibrium ionic configurations for the $\text{Na}_{14}\text{F}_{13}$ cluster, calculated at 100 K using the (b) BH and (c) FT interionic potentials.

lution of the system (at 100 K), the ground- and first three excited-state energies and wave functions are determined,^{11,12} and used to obtain transition energies and dipoles along the trajectory of the system. (It was generally found that these first three excited states carried appreciable transition moments.) Consequently, the calculated electronic absorption spectra reflect the variations in transition energies and transition probabilities for the dynamically generated equilibrium ensemble configurations of the system.¹¹

The $\text{Na}_n\text{F}_{n-1}$ clusters are produced as described previously⁸ by laser vaporization of Na metal into a He flow stream containing approximately 0.01 SF_6 ; the termination of the flow into vacuum results in a supercooled cluster beam (estimated temperature $30 < T < 100$ K), which is size-selectively detected by photoionization time-of-flight spectrometry. Two kinds of spectra (Fig. 3) are obtained: (i) photoionization spectra (bound \rightarrow continuum) using one laser scanned across the above-threshold region; and (ii) photoabsorption spectra, recorded by the resonant two-photon ionization (R2PI) technique, using independent excitation ($h\nu_1 = 1.5$ – 2.6 eV) and ionization ($h\nu_2 = 2.8$ eV) dye lasers. As demonstrated earlier theoretically⁶ and through electron binding and abundance measurements,⁸ class-I clusters attach the electron in a weakly bound surface state; thus $\text{Na}_{14}\text{F}_{13}$ ($3 \times 3 \times 3$) and $\text{Na}_{23}\text{F}_{22}$ ($3 \times 3 \times 5$) exhibit a (continuum) photoionization spectrum above 1.8 eV (Fig. 3, top). In the near-infrared region, absorption bands are located by a series of R2PI mass spectra, such as those shown in Fig. 4 across the 1.2–1.5-eV range.

The computed optical-absorption spectra for Na_2F , Na_4F_3 , $\text{Na}_{18}\text{F}_{17}$, and Na_2Cl , shown in Fig. 1, were ob-

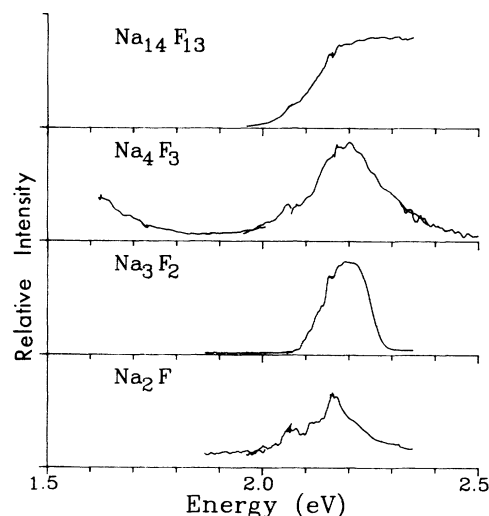


FIG. 3. Optical spectra of the smaller $\text{Na}_n\text{F}_{n-1}$ clusters in the 1.5–2.5-eV region ($n = 2, 3, 4$ are shown in separate frames). The top panel shows the abrupt threshold behavior found for $n = 14$ (the surface state). Note that in the Na_4F_3 cluster, the absorption rises strongly again at low energies (full spectrum below 1.6 eV was not obtained, but see Fig. 4).

tained using two rigid-ion models for the interionic interaction potentials; the Fumi-Tosi¹⁴ (FT) or the Born-Huang¹⁵ models, both parametrized to fit, and widely used in studies of bulk properties of condensed alkali halides. For both the stoichiometric and Cl⁻-deficient alkali chlorides both models yield similar results in satisfactory agreement with experimental data (bond lengths, vibrational frequencies, and structures). The spectrum obtained for Na₂Cl [Fig. 1(d)] is in good agreement with the preliminary measurements of Kappes.¹⁶ Furthermore, in agreement with previous results, the calculated equilibrium geometry of [Na₂Cl]⁺ is linear,¹⁰ with $d_{\text{NaCl}} = (4.62 \pm 0.08)a_0$, and that of Na₂Cl is bent¹⁷ [see Fig. 1(d)]. The calculated values of the electron vertical binding energy, E_c , cluster reorganization energy (the difference between the interionic energies of the neutral and positively charged clusters), E_r , and adiabatic binding energy, $E_a = E_c + E_r$, are (at 100 K) $E_c = 1.36(0.12)$ eV, $E_r = -3.63(0.2)$ eV (values in parentheses denote the calculated standard deviation) compared to the experimental value^{17(b)} $E_a(\text{expt}) = -4.1 \pm 0.1$ eV.

For the small sodium-fluoride clusters the BH potential is found to give superior energetic and spectroscopic results to those obtained with the FT potential. This is not surprising since the FT potential gives a diatomic NaF bond that is too short and too strong compared with experiment. For example, for [Na₄F₃]⁺ the FT optimal structure is a linear chain while that for BH is a distorted cube. Similarly, upon electron attachment the geometries of the Na₄F₃ clusters are a ring (FT) and distorted cube (BH), resulting in very different energetic and optical properties. Calculated (using BH) and measured⁸ values are as follows: For Na₂F: $E_c = 0.83(0.15)$ eV, $E_r = -3.47(0.15)$ eV, $E_a(\text{expt}) = -3.85 \pm 0.15$ eV;

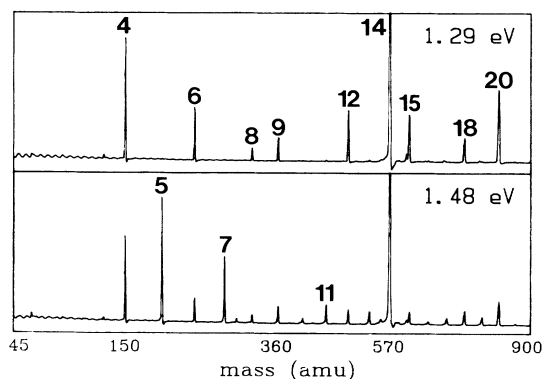


FIG. 4. Two-color R2PI mass spectra: (a) In the 1.23–1.4-eV region, only the clusters designated as surface *F*-center clusters (i.e., class II, see text) exhibit strong absorption. (b) By contrast, at 1.48 eV, the noncubic clusters are the stronger absorbers. Also note that the “two-dimensional clusters” $n=2$ and 3 are transparent in this region. Note that clusters $n=14$ and 23 (and to a much lesser extent, 18) are ionized by the second color alone (2.85 eV), so that no information on these clusters can be obtained from these spectra.

for Na₃F₂: $E_c = 1.41(0.15)$ eV, $E_r = -3.36(0.13)$ eV, $E_a(\text{expt}) = -3.85 \pm 0.15$ eV; for Na₄F₃: $E_c = 0.80(0.15)$ eV, $E_r = -3.27(0.15)$ eV, $E_a(\text{expt}) = -3.54 \pm 0.05$ eV. To demonstrate the effect of temperature on the calculated spectral line shapes we have calculated the spectrum [Fig. 1(b)] for the Na₄F₃ cluster at both 50 and 100 K.

The experimentally observed (see Fig. 3) high-energy absorption band for the three smallest Na_{*n*}F_{*n*-1} clusters [and in others, such as $n=8$ as well, but not in cubic or noncubic (class III) or clusters] is characterized by peak position, width, and shape in satisfactory correspondence with the theoretical predictions. The high-energy band observed for Na₄F₃ is symmetrical and tails off strongly at lower energy, in agreement with the lower-temperature simulation result [Fig. 1(b)], before rising strongly below 1.6 eV, indicating a second lower transition in accord with the theoretical predictions and with the C_{3v} symmetry of this cluster. Additionally, the comparison of the experimental and calculated ionization potential of the Na₄F₃ cluster, using the BH potentials, and the modest reorganization energy (0.8 eV), strongly supports the structure illustrated in Fig. 1(b). The spectrum of Na₃F₂ also exhibits a very sharp band at ~ 2.0 eV. Simulations show that this transition is associated with the excess electron localized at the site of the halide deficiency on a two-dimensional ring. (A lower transition below 1.2 eV is also predicted but not yet found.)

A sensitive test of the theoretical model is obtained for the surface states predicted for the cubic-ion clusters (class I), and characterized experimentally by smaller adiabatic binding energies and instability with respect to atom detachment. The smallest of this class is Na₁₄F₁₃, whose charged parent, [Na₁₄F₁₃]⁺, has an unusually stable $3 \times 3 \times 3$ cubic structure.^{6,10} In this symmetric configuration the electron is distributed uniformly around the cluster. Using the GSD evolution (with the BH interionic potential, at 100 K) the electron rapidly localizes, forming a diffuse surface state [Fig. 2(b)]. This process involves a rather small structural distortion ($E_c = 0.21$ eV). The calculated adiabatic binding energy of the electron is low ($E_a = -1.81$ eV), in excellent agreement with the experimental value⁸ (-1.88 eV) obtained by photoionization spectroscopy (Fig. 3, top), which also shows an abrupt threshold indicative of a very small reorganization energy. The predicted optical spectrum consisting of a single very-low-energy absorption band centered about 0.4 eV [Fig. 2(a)] is very distinct from that of the aforementioned surface *F*-center absorptions (in class-II clusters). (On the other hand, the FT potential yields a surface state [see Fig. 2(c)] with $E_a = -2.22$ eV, a much larger structural rearrangement ($E_c = 1.60$ eV), and a spectrum [Fig. 2(a)] inconsistent with experiment which shows no resonances in the ionization continuum.)

The predicted spectral consequences of different modes of localization have been investigated for the

$\text{Na}_{18}\text{F}_{17}$ cluster ($3 \times 3 \times 4$), which is sufficiently large so that it can possess internal, corner (vertex), face, and edge sites for the excess electron. In the lowest-energy configuration the electron is bound in an F -center surface state, localized at an anion vacancy at the corner of the cubic microcrystal with $E_c = 1.33(0.5)$ eV and $E_a = -2.31(0.15)$ eV [$E_a(\text{expt}) = -2.89$ eV; Ref. 8]. Figure 1(c) illustrates the spectral differences between the corner (C) and interior (I) states, the latter being a long-lived metastable configuration with $E_c = 1.84(0.2)$ eV and $E_a = -1.34(0.2)$ eV. The interior state is characterized by a single broad feature peaking near 2.2 eV [Fig. 1(c)], well below the experimental value for an F center in a bulk sodium-fluoride crystal¹⁸ (3.64 eV), thus emphasizing the importance of long-range interactions. The corner state, by contrast, exhibits a spectrum very similar to that of Na_4F_3 , indicating dominance of local symmetry and interactions in determining the nature of such surface F -center states. Similar but distinct spectra are predicted for other long-lived metastable surface states in which the electron is localized at an anion vacancy on the edges ($E_a = -1.85$ eV) or on the faces ($E_a = -1.61$ and -1.49 eV, for the 3×3 and 4×3 faces, respectively) of the microcrystalline cluster.

In agreement with these predictions, scans covering the full 1.25–1.6-eV spectral range have revealed characteristic absorption bands for the larger clusters ($n < 33$), except the cubic ions (14 and 23). Figure 4 provides qualitative indications of the distinct characteristics associated with each type of localization mode. We associate the strong infrared absorption (1.25 eV), found only for the surface F -center (class II) clusters ($n > 3$, $n = 4, 6, 8, 9, 12, 15, 18, 20, 24, \dots$, see Ref. 8; values are slightly different for chlorides^{10,19}) with the corner-site localization found for Na_4F_3 [Fig. 1(b)] and $\text{Na}_{18}\text{F}_{17}$ [Fig. 1(c)], although it appears to peak at somewhat lower energy than predicted by theory. At 1.48 eV, by contrast, the absorption of surface F -center clusters is much weaker than the noncubic clusters, as is made clear by comparison with the reference abundance spectrum [see Fig. 1(a) in Ref. 8]. No bands are detected in the 1.25–2.0-eV range for class-I cubic-ion clusters ($n = 14$ and 23) or for two-dimensional clusters ($n = 2$ and 3).

It will be of interest to extend the experimental and theoretical investigations to larger clusters and to F -center defects at ionic crystalline surfaces, in order to examine further the suggested characteristic spectral distinction between bulk, surface F -center, and diffuse surface excess electron states. Additional information can be obtained from the vibrational spectral shifts associated with the electron attachment,^{3(b)} which exhibit softening of stretch modes due to partial screening of cations and stiffening of bending modes in the vicinity of the excess electron.

We thank Dr. Manfred Kappes for providing the Na_2Cl spectrum prior to publication. Work at Georgia

Institute of Technology supported by U.S. DOE Grant No. FG05-86ER45234, at University of California, Los Angeles, by the Office of Naval Research, and at Tel Aviv by the Israel Academy of Science and by the U.S.–Israel Binational Science Foundation.

^(a)Permanent address: School of Chemistry, Sackler Faculty of Science, Tel Aviv University, Tel Aviv 69978, Israel, and Department of Chemical Physics, The Weizmann Institute of Science, Rehovot, Israel.

^(b)Also with Department of Physics.

^(c)Permanent address: Laboratoire de Spectrometrie Ionique et Moleculaire (CNRS 171), Universite Lyon I, Villeurbanne, France.

¹M. M. Kappes and S. Leutwyler, in *Atomic and Molecular Beam Methods*, edited by G. Scoles (Oxford Univ. Press, London, 1989).

²R. L. Whetten and M. Y. Hahn, in *Atomic and Molecular Clusters*, edited by E. R. Bernstein (Elsevier, New York, 1989).

³For recent reviews, see (a) R. N. Barnett, U. Landman, D. Scharf, and J. Jortner, *Acc. Chem. Res.* **22**, 350 (1989); J. Jortner, D. Scharf, and U. Landman, in *Elemental and Molecular Clusters*, edited by G. Benedek, T. P. Martin, and G. Pacchioni (Springer-Verlag, Berlin, 1989), p. 148; (b) R. N. Barnett, U. Landman, Gunaretnam Rajagopal, and A. Nitzan, *Isr. J. Chem.* (to be published).

⁴For review, see P. J. Rossky and J. Schnitker, *J. Phys. Chem.* **92**, 4277 (1988).

⁵R. N. Barnett, U. Landman, and A. Nitzan, *Phys. Rev. Lett.* **62**, 106 (1989); L. A. Posey *et al.*, *J. Chem. Phys.* **91**, 6536 (1989).

⁶U. Landman, D. Scharf, and J. Jortner, *Phys. Rev. Lett.* **54**, 1860 (1985).

⁷D. Scharf, U. Landman, and J. Jortner, *J. Chem. Phys.* **87**, 2716 (1987).

⁸E. C. Honea, M. L. Homer, P. Labastie, and R. L. Whetten, *Phys. Rev. Lett.* **63**, 394 (1989).

⁹Y. A. Yang, C. W. Conover, and L. Bloomfield, *Chem. Phys. Lett.* **158**, 279 (1989).

¹⁰T. P. Martin, *Phys. Rep.* **95**, 167 (1983).

¹¹R. N. Barnett, U. Landman, and A. Nitzan, *Phys. Rev. A* **38**, 2178 (1988); *J. Chem. Phys.* **89**, 2242 (1988), and references therein. See also Ref. 3.

¹²See review by R. Kosloff, *J. Phys. Chem.* **92**, 2087 (1988).

¹³D. Scharf, J. Jortner, and U. Landman, *Chem. Phys. Lett.* **130**, 504 (1986).

¹⁴F. G. Fumi and M. P. Tosi, *J. Phys. Chem. Solids* **25**, 31 (1964); **25**, 45 (1964).

¹⁵M. Born and K. Huang, *Dynamical Theory of Crystal Lattices* (Oxford Univ. Press, London, 1954).

¹⁶M. Kappes (private communication).

¹⁷(a) G. Galli, W. Andreoni, and M. P. Tosi, *Phys. Rev. A* **34**, 3580 (1986); (b) K. I. Peterson, P. D. Dao, and A. W. Castelman, Jr., *J. Chem. Phys.* **79**, 777 (1983); M. Kappes, P. Radi, M. Schar, and E. Schumacher, *Chem. Phys. Lett.* **113**, 243 (1985); (c) T. M. Miller, D. G. Lepold, K. K. Murray, and W. C. Lineberger, *J. Chem. Phys.* **85**, 2368 (1986).

¹⁸C. C. Klick, in *American Institute of Physics Handbook* (McGraw-Hill, New York, 1972), 3rd ed., pp. 9–148.

¹⁹R. Pflaum, K. Sattler, and E. Recknagel, *Chem. Phys. Lett.* **138**, 8 (1987).

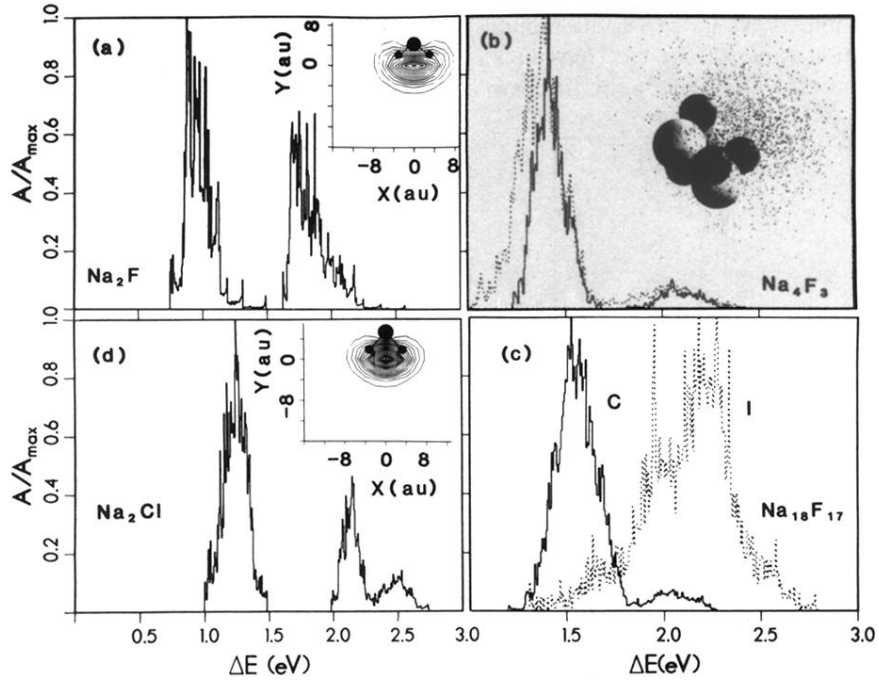


FIG. 1. (a),(b) Calculated spectra for Na_2F (at 100 K) and Na_4F_3 , respectively, using the BH potentials. (b) For Na_4F_3 spectra calculated at 100 K (dashed curve) and 50 K (solid curve) are shown. Insets: (a) Contours of the excess electron density (maximum contour corresponds to $3.089 \times 10^{-3} e/a_0^3$ and the increment between successive contours $\Delta = 2.56 \times 10^{-4}$) in the plane of the Na_2F molecule, and (b) a snapshot of the equilibrium configuration at 100 K of the Na_4F_3 cluster, where the large and small balls correspond to F^- and Na^+ ions, respectively, and the excess electron distribution is represented by the small dots. The geometry of the Na_2F cluster is specified by $d_{\text{Na-F}} = (3.71 \pm 0.11)a_0$, $\theta(\text{Na-F-Na}) = 110.5^\circ \pm 4.0^\circ$, and the distance between the fluorine anion (large filled circle) and the center of the excess electron density $d_{\text{F-e}} = (4.28 \pm 0.15)a_0$. (c) Calculated excess electron spectra for two configurations of the anion vacancy [internal (*I*), dashed curve; corner (*C*), solid curve] of $\text{Na}_{18}\text{F}_{17}$ at 100 K. (d) Calculated spectrum for Na_2Cl at 100 K, using the FT potentials. Inset: Contours of the excess electron density (maximum contour $4.35 \times 10^{-3} e/a_0^3$, $\Delta = 2.724 \times 10^{-4}$). The structural parameters are $d_{\text{NaCl}} = (4.73 \pm 0.09)a_0$, $\theta(\text{Na-Cl-Na}) = 85.7^\circ \pm 2.9^\circ$, and $d_{\text{Cl-e}} = (5.39 \pm 0.08)a_0$.

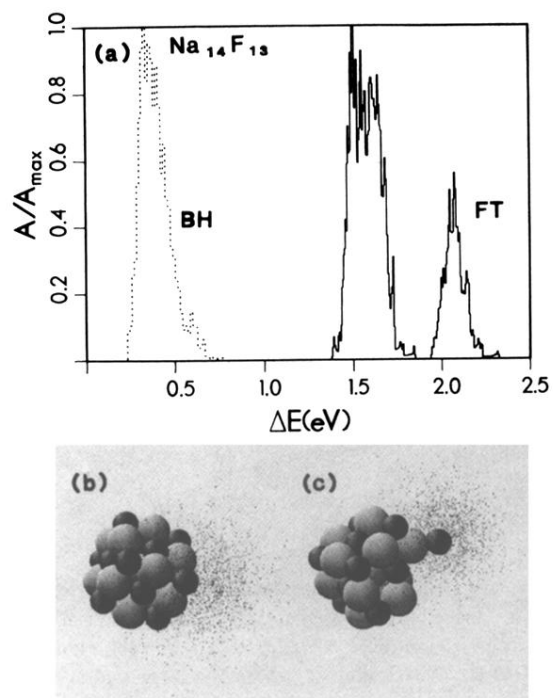


FIG. 2. (a) Calculated spectra for an excess electron surface state in an $\text{Na}_{14}\text{F}_{13}$ cluster at 100 K. Results obtained via the BH and FT potentials are given by dashed and solid curves, respectively. (b),(c) Snapshots of equilibrium ionic configurations for the $\text{Na}_{14}\text{F}_{13}$ cluster, calculated at 100 K using the (b) BH and (c) FT interionic potentials.